International Journal of Engineering Research & Technology (IJERT)
ISSN: 2278-0181
Vol. 15 Issue 02 , February - 2026

Characterization and Performance Analysis of Fabricated PDMS and ZnO/PDMS Based Piezoelectric Pressure Sensor

R. Ananthi, Dr. P. Thirumoorthy
[1]Department of Electronics and Communication, Government Arts College, Dharmapuri, Affiliated to Periyar University, Salem – 636 011, Tamil Nadu, India.

Dr. K.A. Ramesh kumar, Dr. P. Maadeswaran
[2]Department of Energy Science and Technology, Periyar University, Salem – 636 011, Tamil Nadu, India.

Paramaguru PV
[3]Department of Electronics And Instrumentation, Bharathiar University, Coimbatore, Tamil Nadu, India.

Abstract - The fabrication of pressure sensor undergoes with different weight percentages of ZnO nanoparticle have maximum β-phase content obtained when composited with PDMS polymer matrix to form ZnO/PDMS nanocomposites while compared with other wt. % ratios. The β-phase of ZnO/PDMS has been increased from 38.2% to 66.1%without requirement of any further processes. The sensors fabricated from ZnO/PDMS- ZnO (15wt. %) gives an output of 2.35v (open circuit voltage) and 0.38μA (short circuit current) with an instantaneous output power density of 0.21 μW/cm2. Then the mask design of the pressure sensor was presented in order to fabricate the mask for pressure sensor development. In order to compensate offset voltage and to obtain 4-20 mA response, the design, fabrication and testing were carried out. The operation of this circuit was demonstrated using a commercial pressure sensor which was not having its own signal conditioning circuit. The performance parameters are investigated in terms of the sensitivity, offset voltage, offset drift, linearity and hysteresis. The developed sensors showed very good linearity, low offset voltage drift and low hysteresis. The effect of elevated temperatures on these parameters was also studied. The pressure sensor sensitivity showed reduction of 13.80 % at 100 ºC for PDMS and reduction of 19.51 % at 200 ºC for ZnO/PDMS based pressure sensor. It can be clearly seen that the ZnO/PDMS based process has a clear advantage for extending the operating range beyond that for commercial standard sensors.

INTRODUCTION

Pressure sensors have a broad range of applications in the several areas such as process control instrumentation in manufacturing industries, oil & gas, automotive, space, medical, etc. Micro-electro-mechanical-systems (MEMS) technology has played a significant role in the evolvement of miniaturised pressure sensors along with integration of microelectronics. For industrial applications, there are two major categories of pressure sensors, firstly based on piezoresistive transduction technique and secondly, based on capacitive transduction technique. Simplicity of fabrication, simple signal conditioning electronics, linearity and accuracy in pressure measurement are most preferred attributes of MEMS technology based piezoresistive pressure sensors[1-8]. The MEMS technology for the fabrication of such pressure sensors for normal operating conditions has been well established.

The piezoelectric properties of ZnO/PDMS active material have to increase for the piezoelectric pressure sensors and the different approaches to increase in β-phase content in PDMS been discussed. Also β-phase has the high polar crystalline-electroactive nature which compared to other phases present in ZnO/PDMS, the nucleation of β-phase is essential for using ZnO/PDMS for pressure sensing devices [10– 13]. The piezoelectric properties of PDMS can be enhanced by adding functional nanomaterials such as TiO 2 [4], Fe-RGO [5], BiVO 4 [14] to disrupt the structural properties of PDMS which results to the nucleation of β-phase. Also, the fundamental nanomaterial with high piezoelectric properties like PZT has been incorporated into the PDMS to increase the overall piezo-response (i.e., from β-phase as well as from the piezoelectric response of the material) of the composite material [15]. However, mainly due to the toxicity and complex preparation method, it is hardly use as a nanofiller in PDMS. The synthesis of ZnO/PDMS based nanocomposite films and the results which investigates the effects on introducing the ZnO nanostructures on the PDMS and its enhanced piezoelectric property [16]. The different Wt. % of ZnO nanoparticles are introduced into the PDMS matrix and it is found that the β-phase content of ZnO/PDMS nanocomposite improved from 48.2% to 76.1% by incorporating ZnO nanoparticles into ZnO/PDMS without any requirement of further processes. The XRD, FTIR, and P-E loop measurements confirmed the increase in β -phase content. It is important to study the role of ZnO having piezoelectric property, since adding it to PDMS has been linked to improving the β-phase and its contribution to the overall performance of the piezoelectric pressure sensor fabricated from ZnO/PDMS based nanocomposite film [17-20].

Design optimisation and simulation study for the piezoresistive pressure sensor was presented in the earlier Chapter. In this Chapter, layout design is presented to fabricate masks for the piezoresistive pressure sensors. Moreover, development of signal conditioning circuit for pressure sensors is described for compensation of offset voltage and to obtain current response in 4-

International Journal of Engineering Research & Technology (IJERT)
ISSN: 2278-0181
Vol. 15 Issue 02 , February - 2026

20 mA. The performance of pressure sensors fabricated in this work in terms of sensitivity, offset voltage, offset drift, linearity, and hysteresis was investigated. The effect of operating temperature on the sensitivity was also studied. The fabrication process was first optimized for diffused resistor pressure sensors as there were many process steps which were common with the SOI technology based sensors. Using the optimized process steps, the fabrication process for SOI based sensors was further optimized.

Methods and fabrication process

Fabrication process development for piezoelectric pressure sensors. The device layer was separated by a thin (~1 µm) PDMS and ZnO/PDMS layer from the handle layer. The handle layer was etched to realize the diaphragm. Moreover, thickness of the device layer was reduced using oxidation process and subsequent etching of oxide layer. In this section discusses, the fabrication process flow for piezoelectric based pressure sensor.

Fabrication process for piezelectric based pressure sensor

Preparation of ZnO/PDMS polymer flexible nanocomposite film Figure 1 depicts the schematic diagram of the various steps involved in the synthesis of ZnO/PDMS nanocomposite films. Adding the prepared ZnO with PDMS compound A and mix with curing agent compound B in the ratio of 10:1 by using doctor blade method and outgassed for 1Hrs at room temperature under vacuum [23-27]. The composite was curing at 70°C for 24Hrs. afterward, the ZnO nanoparticles are added into the ZnO in different weight percentages of 15wt. %, of size 1.5cm × 1.5cm as mentioned above. After this, we let the film cool down for a few Hrs. We dip the substrate with film into deionized water at room temperature. The film peels off from the substrate easily. No water gets stick on them because of the hydrophobic nature of the films. We have used these free-standing films (1.5cm × 1.5cm × 60µm) shown in Figure 1 for fabricating the Nano generator.

Fabrication of the piezoelectric pressure sensor

To explore the potential of the ZnO/PDMS flexible polymer nanocomposite films for use in pressure sensing, we fabricated the piezoelectric sensors from the films, as shown in Figure 2. For the fabrication of device from the free-standing nanocomposite films, first, a chromium layer of thickness 10nm, then a copper layer of thickness 50nm is deposited on both sides of the film by Thermal Evaporation Deposition. From the metal electrode, electrical wires are connected using silver paste for measurement. The system is encapsulated with an insulating tap so that when we impart pressure, the metal electrodes remain untouched. On both sides of the film, the total active electrode area is 1.5cm × 1.5cm. Then the performance investigations of pressure sensor was studied by carrying out various measurements after final assembly.

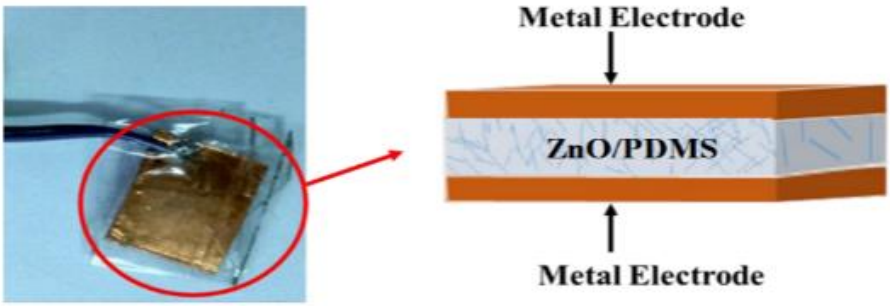

Figure:1 Photographic and cross-section diagram of the fabricated piezoelectric pressure sensor. Further, metallisation is carried out to connect the piezoelectric based samples in Wheatstone bridge configuration.

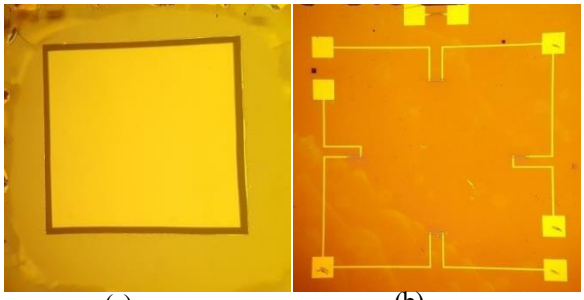

(a) (b)

Figure 2 (a) Bottom view of fabricated area, (b) Top view of fabricated area.

International Journal of Engineering Research & Technology (IJERT)
ISSN: 2278-0181
Vol. 15 Issue 02 , February - 2026

Signal Conditioning Circuit

The pressure sensor converts non-electrical signal, i.e. pressure, into electrical signal, i.e. voltage. However, the electrical output of the sensors needs further amplification. Therefore, a signal conditioning circuit is needed for amplification of pressure sensor output to a suitable voltage or current level for further processing. The Wheatstone bridge on the top of the thin diaphragm is one of the most used techniques to convert pressure signal into the electrical signal. The resistances of Wheatstone bridge piezoelectric (resistant compensation) are not identical which leads to the offset voltage. A suitable compensation technique is required to compensate the offset voltage. Design, fabrication and experimental evaluation of the signal conditioning circuit were carried out for offset compensation, output amplification and to obtain 4 to 20 mA output response. The 4-20 mA current response is highly immune to external noise and hence is an industry standard.

Analysis and modelling of Wheatstone bridge for offset voltage compensation

A piezoelectric pressure sensor is fabricated using the DC sputtering and nano filled PDMS substrates having its piezoresistance on the top of thin diaphragm. The output of the bridge must be zero under unstressed condition and it must also remain zero for other any temperature because all four resistors have the same temperature coefficients. However, in practice there is always a non zero voltage output under the unstressed condition. The non-zero output is referred to as the offset voltage of the piezoelectric pressure sensor. The main possible reasons for offset voltage are [30]:

1. Geometrical deviation of resistors from their nominal values.
2. Initial stresses in the diaphragm due to the thermal mismatch of the piezoelectric layer and PDMS substrate.
3. Non-identical temperature dependency of piezoresistance.

Here, analytical modelling of the offset voltage and temperature coefficient of offset (TCO) is presented. We consider that all four piezoresistors are identical and equal to the nominal resistance $R_1 = R_2 = R_3 = R_4 = R_b$ as shown in Figure 3.

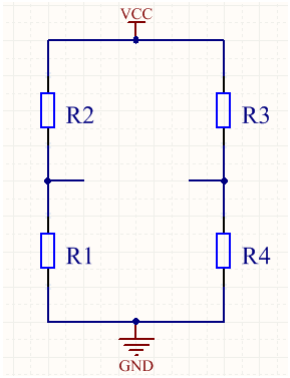

Figure:3 Wheatstone bridge configuration.

Also, we assume that each resistance has some deviation from the nominal resistance value, i.e. $R_1 = R_b(1+\delta_1), R_2 = R_b(1+\delta_2), R_3 = R_b(1+\delta_3), and\ R_4 = R_b(1+\delta_4)$.

$$V_{offset} = V_{01} - V_{02} = \frac{R_1R_3 - R_2R_4}{(R_1+R_2)(R_3R_4)}V_{cc} = \left(\frac{\delta_1}{4} + \frac{\delta_3}{4} - \frac{\delta_2}{4} - \frac{\delta_4}{4}\right)V_{cc}, V_{offset} = \left(\frac{\delta_1}{4}\right)V_{cc} \quad (1)$$

Where, $\frac{\delta}{4} = \frac{\delta_1}{4} + \frac{\delta_3}{4} - \frac{\delta_2}{4} - \frac{\delta_4}{4}$

The offset voltage is not temperature dependent if and only if all the resistors have the same temperature coefficient of resistance. It is difficult to get an identical temperature coefficient for all piezoelectric samples [35]. Hence, the compensation of offset voltage is essential task before signal conditioning. The configuration for the offset compensation is presented in (Figure 4 (a) –(c)).

International Journal of Engineering Research & Technology (IJERT)
ISSN: 2278-0181
Vol. 15 Issue 02 , February - 2026

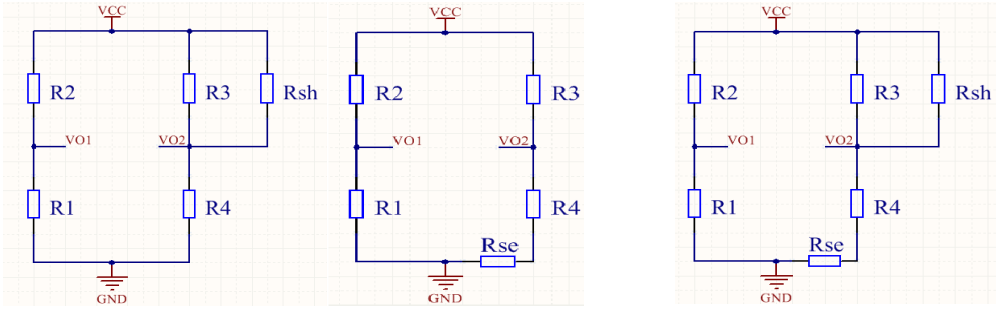

(a) (b) (c)

Figure 4: Compensation techniques; (a) parallel (b) series (c) parallel-series.

The offset compensation is usually done by a passive resistor component in the parallel or series configuration. In order to make offset voltage less temperature dependent, the passive resistor is to be selected with a smaller temperature coefficient than the piezoelectric samples. Mathematically, the required value of selected resistor for offset compensation is calculated as explained in the consecutive sections.

Offset compensation using a parallel configuration

The compensation resistor is utilised to tune the value as per the desired nominal resistance [35]. Hence, resistance of parallel configuration is equal to nominal resistance, R_b (Figure 4 (a)).

$$\frac{R_3 + R_{sh}}{R_0 + R_{sh}} = R_b \frac{R_b(1+\delta_3)R_{sh}}{R_b(1+\delta_3)+R_{sh}} = R_b$$

$$\delta_3 + R_{sh} = R_b + R_b\delta_3$$

$$R_{sh} = \frac{R_b}{\delta_3}$$

Generally, TCR is defined as;

$$TCR = \frac{R_t - R_0}{R_0}\frac{1}{T_t - T_0}$$

$$TCR_{R_3 \| R_{sh}} = \frac{R_{3t} \| R_{sh} - R_0 \| R_{sh}}{R_0 \| R_{sh}}\frac{1}{T_t - T_0}$$

$$TCR_{R_3 \| R_{sh}} = \frac{R_{sh}}{R_0 + R_{sh}} TCR_3$$

Where, $R_3 \| R_{sh}$ is the parallel configuration of the resistors and TCR_3 is TCR for piezoelectric $R3$. Due to the parallel configuration effective "Temperature coefficient of Resistance" (TCR) is reduced as shown in the above equation.

Offset compensation using series configuration

The compensation resistor is utilised to tune the value as per the desired nominal resistance [35]. Hence, the resistance of series configuration should be equal to the nominal resistance (Figure 4(b)).

$R_4 + R_{se} = R_b$ or $R_b (1+ \delta_4) + R_{se} = R_b$

$R_{se} = -\delta_4 R_b$

The effective temperature coefficient of resistance (TCR_{eff}) is calculated for series configuration as;

$$TCR_{R_3+R_{se}} = \frac{(R_{4t}+R_{se})-(R_0+R_{se})}{R_0+R_{se}}\frac{1}{T_t-T_0} \quad \text{OR} \quad TCR_{R_3+R_{se}} = \frac{R_{4t}-R_0}{R_0+R_{se}}\frac{1}{T_t-T_0}$$

Hence, the effect of the TCR due to the Wheatstone bridge resistance is reduced due to external passive components as shown in the above equations.

Offset compensation using parallel-series configuration

Offset compensation of the piezoresistive pressure is done using parallel-series compensation technique [35].

International Journal of Engineering Research & Technology (IJERT)
ISSN: 2278-0181
Vol. 15 Issue 02 , February - 2026

The parallel-series configuration is given in Figure 4(c).

Design and testing of signal conditioning circuit

As per industrial standards, the response of pressure sensor is calibrated in terms of 4 to 20 mA current for zero and maximum applied pressure respectively. Based on the requirements of pressure sensor output signal processing, a survey was conducted for various ICs suitable for the application. The IC XTR105 by Texas Instruments Inc. was identified for the development of the electronics. The schematic of the signal conditioning circuit is shown in Figure 4.10. A layout of circuit was made, the PCB was fabricated and fabricated PCB was assembled with required components (Figure 5).

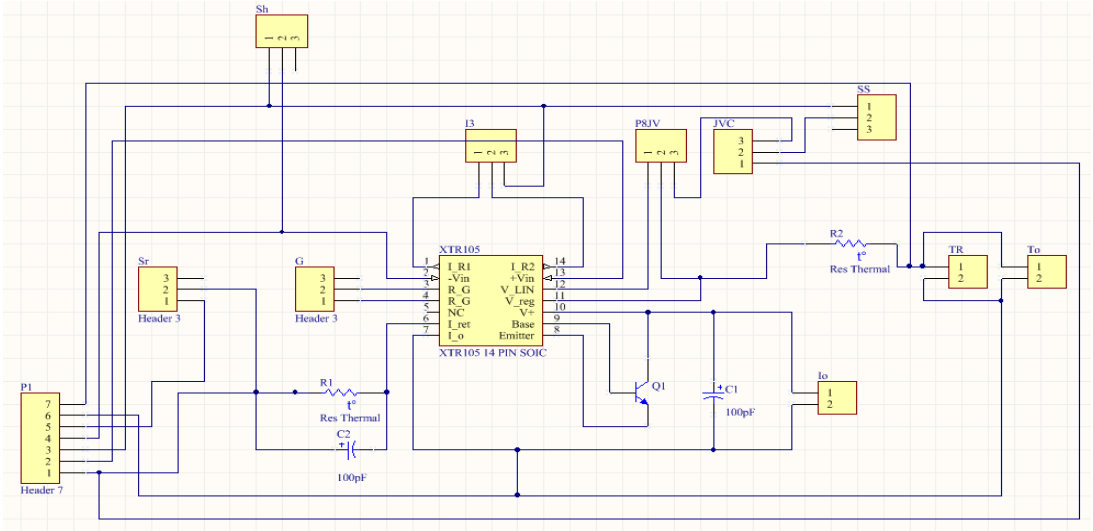

Figure 5: Schematic of the signal conditioning circuit for obtaining 4 to 20 mA current loop response.

The designed circuit has features such as; i) possibilities for the compensation of offset voltage by one of the three configurations as discussed above, ii) amplification of sensors output, iii) constant voltage or constant current supply source. Finally, the designed and fabricated signal conditioning circuit was tested for 4 to 20 mA current output and offset voltage compensation using a pressure sensor. The sensor was characterised with and without offset compensation. The testing results of the developed signal conditioning circuits are presented for compensation of offset voltage. The output voltage was recorded for uncompensated and compensated case using a commercial pressure sensor.

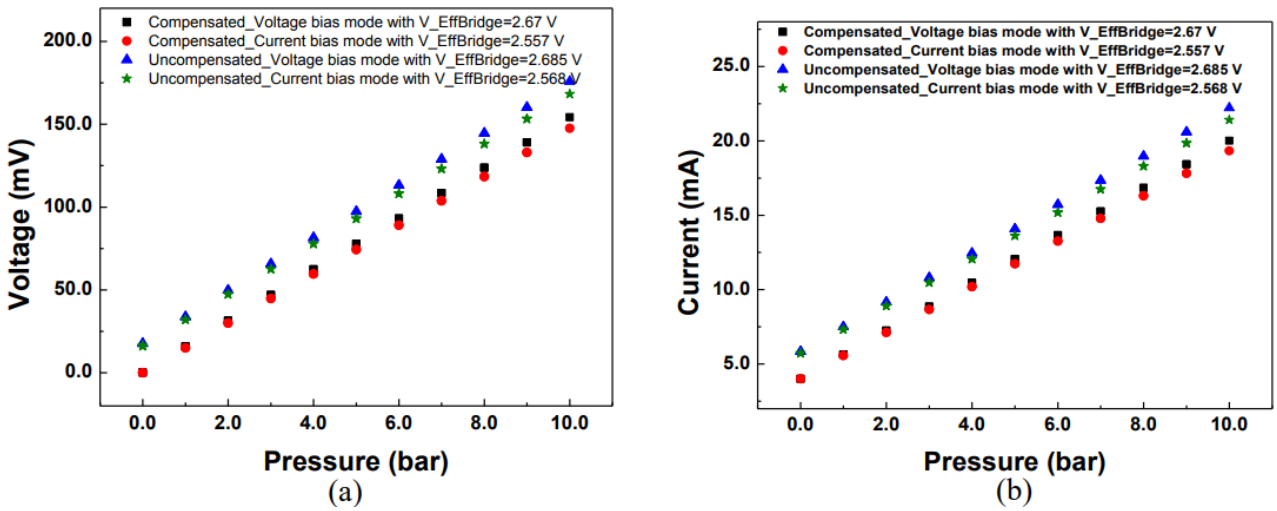

Figure 6: (a) Voltage response of pressure sensors for uncompensated and compensated conditions, (b) The 4-20 mA current response for uncompensated and compensated conditions.

The compensation of offset voltage was successfully achieved using the developed signal conditioning circuit in both the supply modes i.e. constant current source and constant voltage source. The results of testing of the circuit are presented in Table 1.

International Journal of Engineering Research & Technology (IJERT)
ISSN: 2278-0181
Vol. 15 Issue 02 , February - 2026

Table 1Results of testing of signal conditioning circuit.

Resistance	R_t	R_{12}	R_{23}	R_{34}	R_{54}	R_b	Effective supply voltage (V)	Voltage at series-shunt Resistor (V)	$\frac{Compensated\ resistance}{R_{sh}\ (k\Omega)}$	$R_{se}\ (\Omega)$	Remark
	kΩ	kΩ	kΩ	kΩ	kΩ	kΩ					
Uncompensated	13.75	3.42	3.48	3.39	3.47		2.685	2.359	NA	NA	
Compensated	13.65	3.46	3.39	3.47	3.41	3.43	2.677	2.359	132.3	~2	Parallel
	13.72	3.49	3.40	3.45	3.39	3.45	2.695	2.359	∞	90.39	Series
	13.63	3.46	3.39	3.39	3.39	3.41	2.675	2.374	148.9	11.26	Series-Parallel

The performance of pressure sensors fabricated in this work in terms of sensitivity, offset voltage, offset drift, linearity, and hysteresis was investigated. The effect of operating temperature on the sensitivity was also studied. The fabrication process was first optimized for diffused resistor pressure sensors as there were many process steps which were common with the ZnO and ZnO/PDMS based sensors. Using the optimized process steps, the fabrication process for sensors was further optimized.

Characterisation Setup

In order to investigate the performance of the pressure sensors, a characterisation setup comprising the following units was built:

- Pneumatic pressure pump and pressure hose in order to apply the pressure.
- Multipurpose calibrator with a reference pressure sensor, power supply and recording instrument to calibrate the pressure sensor under investigation.
- Digital multi-meter for the measurement of the surface resistance of piezoelectric device.
- Temperature environment chamber with a temperature controller to perform the experiment under elevated temperatures.

The multipurpose calibrator was used as a data logger and calibrator for pressure sensor response. The calibrator was also used to power up the pressure sensor. A pneumatic pressure pump was used to pressurise the pressure sensor under test. The pneumatic type of pressure was selected in order to keep the chip isolated from the moisture and vapour particles, which can come from the hydraulic kind of the pressure pump. This was required a s the packaging of the developed prototype of pressure sensors did not have stainless steel diaphragm for isolation in between the sensor chip and pressure media. In addition, a high-resolution multimeter was used to precisely measure the bridge resistance of the pressure sensor. Moreover, an in-house designed and developed temperature chamber with the controller was utilised in order to investigate the effect of temperature on the pressure response. The schematic and actual photograph of pressure sensor characterisation setup is presented in Figure 7 respectively.

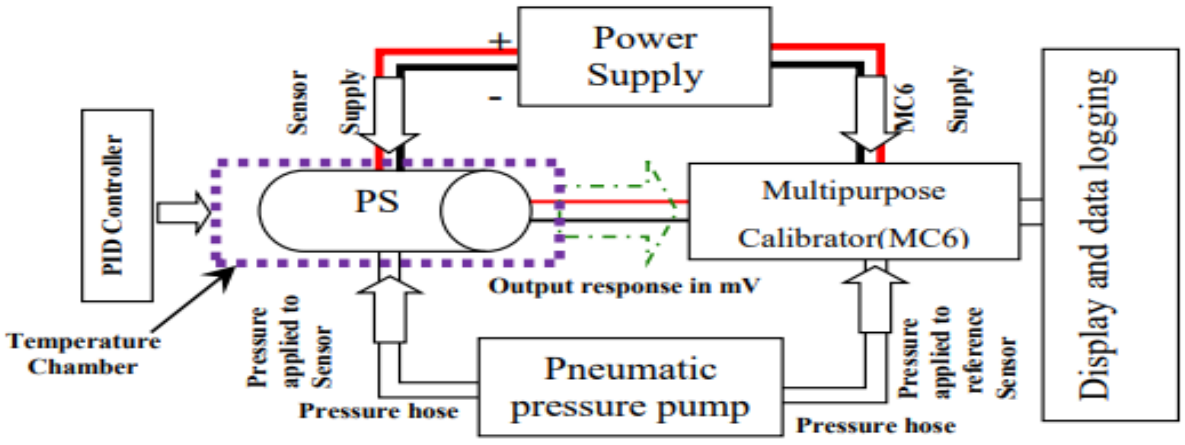

Figure 7: (a) Schematic of the pressure sensor characterization setup

Results and discussion

Performance study of pressure sensors fabricated during process development. The typical performance results for (a) PDMS based, and (b) ZnO/PDMS based piezoelectric pressure sensors at different temperatures are presented.

International Journal of Engineering Research & Technology (IJERT)
ISSN: 2278-0181
Vol. 15 Issue 02 , February - 2026

Pressure response with Offset

The pressure response of diffused resistor and SOI based fabricated piezoelectric pressure sensors was measured at different temperatures and analysed. The temperature induced variation in the response was obtained after subtracting the offset of the pressure sensors. The response of the pressure sensor is shown for diffused and SOI technology based pressure sensor in Figure 8 (a) and (b). Since all resistors were not identical, it resulted in a considerable output voltage at no pressure conditions i.e. offset voltage.

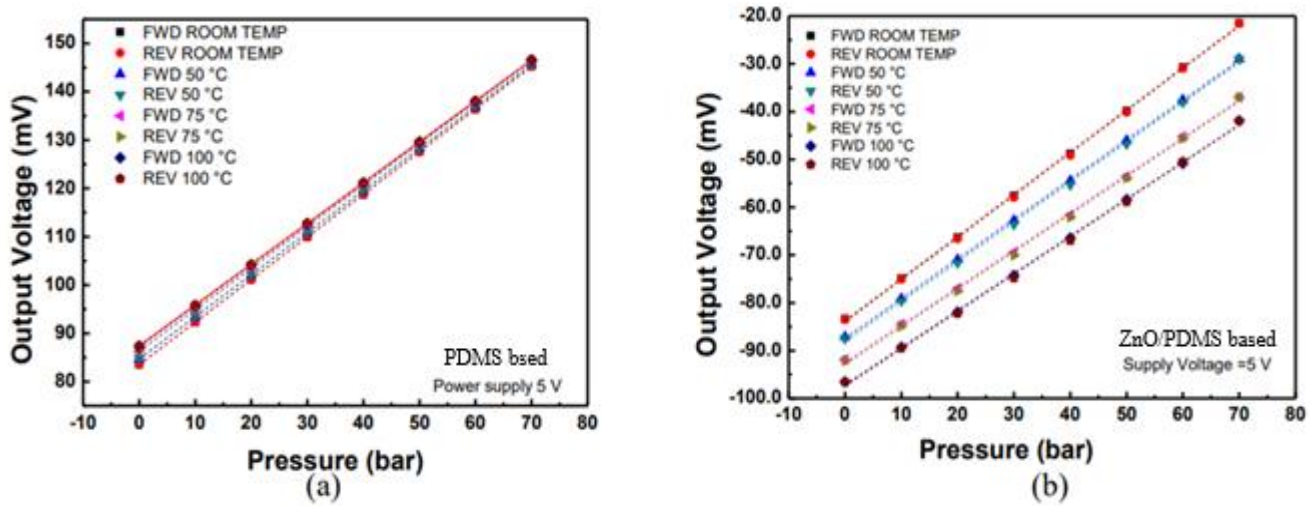

Figure 8: Pressure response under the elevated temperatures for (a) Passivated PDMS based and (b) ZnO/PDMS based pressure sensor with 150 µm diaphragm thickness and 100 bar pressure range.

It is observed that the change in the sensitivity of ZnO/PDMS based pressure sensor is less as compared to the PDMS based pressure sensor. It can be attributed to the higher doping concentration of ZnO in PDMS thin film based pressure sensors.

Sensitivity

The sensitivity is defined the slope of the plot between output voltage vs input pressure. Sensitivity of the pressure sensor was observed to degrade by ~ 4.5 % and ~ 14 % for the developed pressure sensors at 100 °C. The measured and calculated sensitivities using a linear curve fitting (slope) are identical and are 0.088 mV/bar at 5 V supply. The concentration of Zn was higher for sensors than for the other type based sensors. Hence a lower change (~4.5 %) is observed for diffused piezoresistor based pressure sensor compared to PDMS based sensor (~14 %). The degradation in the sensitivity under temperature for ZnO/PDMS based pressure sensor is depicted in Figure 9 (a) and (b) (measured) and Figure 10 (a) and (b) (linear fit).

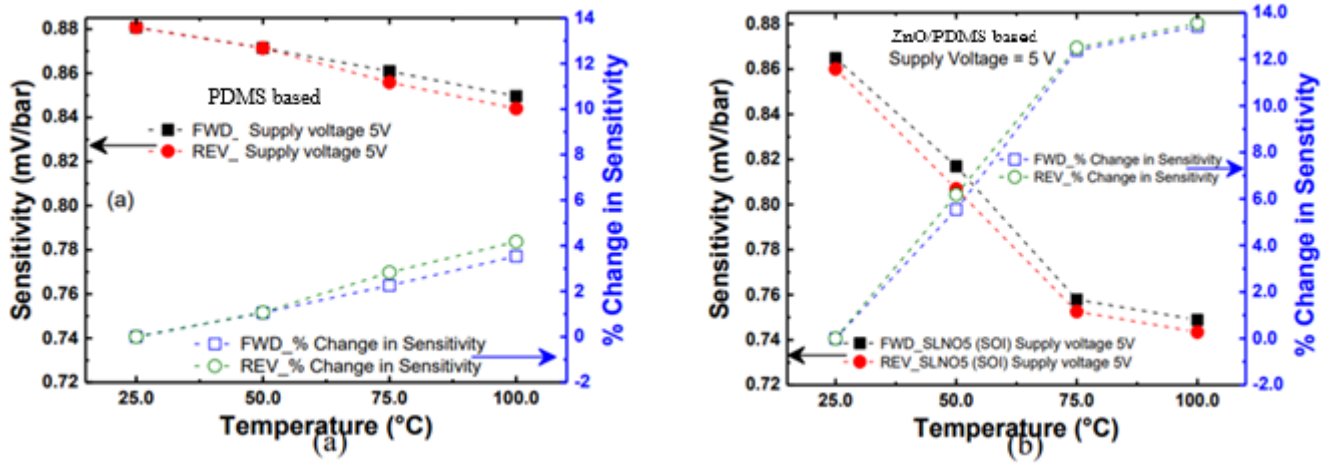

Figure 9: Sensitivity and % degradation of sensitivity for pressure sensors (a) PDMS based, and (b) ZnO/PDMS based.

International Journal of Engineering Research & Technology (IJERT)
ISSN: 2278-0181
Vol. 15 Issue 02 , February - 2026

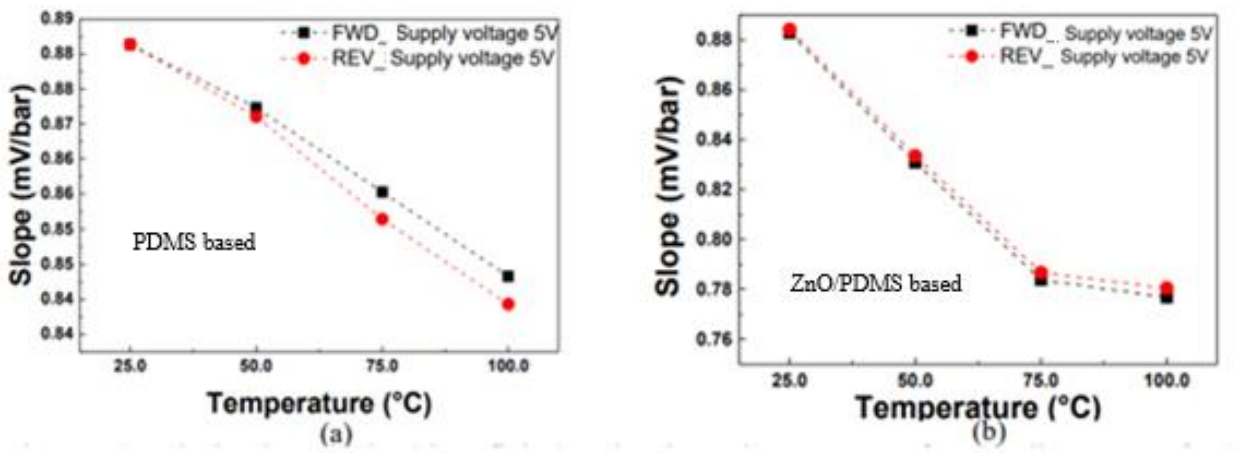

Figure 10: Calculated sensitivity (slope fitting) under elevated temperatures from the linear curve for (a) PDMS based, and (b) ZnO/PDMS based sensor respectively.

ZnO/PDMS based sensors have piezoresistance isolated from the surface by coated ZnO layer. However, since piezoresistive coefficient decreases with increase of temperature, the sensitivity is observed to decrease. Due to hysteresis, the sensitivities are different in forward and reverse characterization for both types of sensors.

Offset voltage

The offset voltage of both pressure sensors was recorded under elevated temperature environments. The maximum degradation was observed as ~5 % and 16 % for PDMS based, and ZnO/PDMS based pressure sensor respectively (Figure 11 (a) and (b)). Moreover, the offset voltage obtained after linear fitting of the data is plotted as shown in Figure 12 (a) and (b).

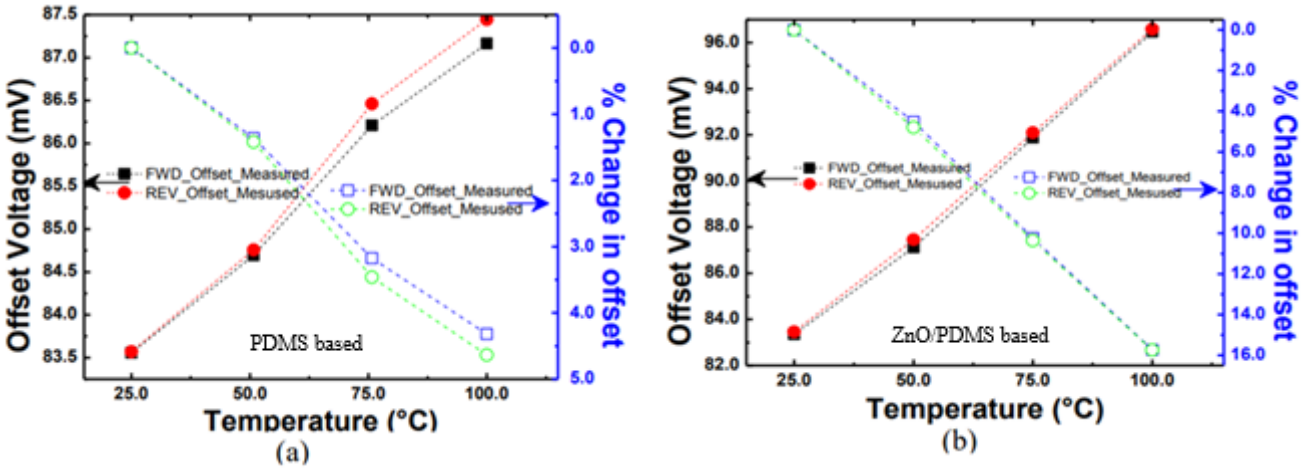

Figure 11: Variation in the offset voltage under elevated temperatures for (a) PDMS based, and (b) ZnO/PDMS based pressure sensor.

International Journal of Engineering Research & Technology (IJERT)
ISSN: 2278-0181
Vol. 15 Issue 02 , February - 2026

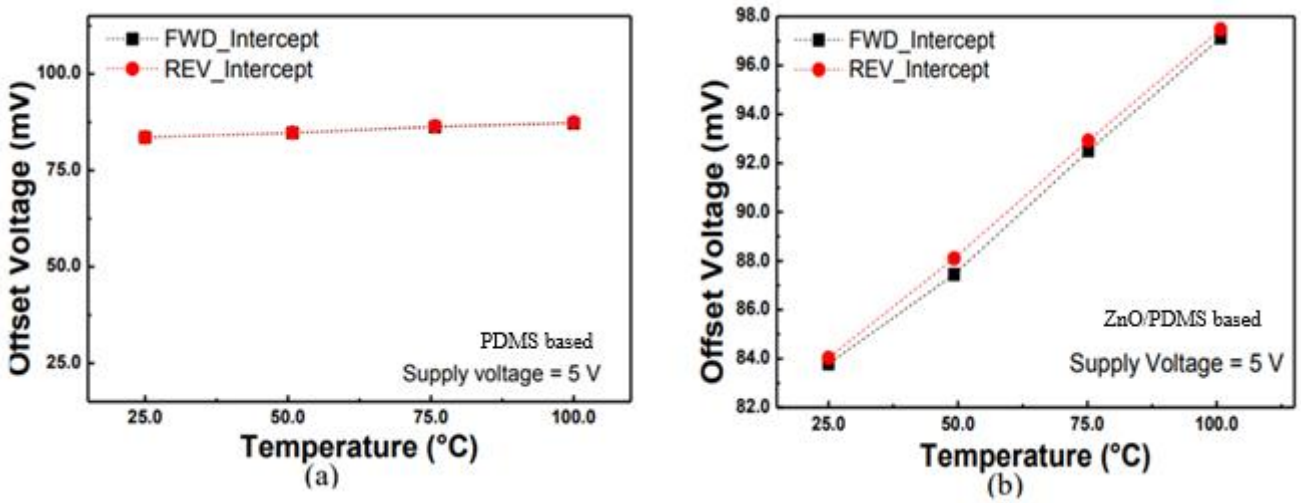

Figure 12: Variation in offset voltage under elevated temperatures for (a) PDMS based, and (b) ZnO/PDMS based pressure sensor using a linear curve fitting.

Offset voltage drift

The drift in offset voltage was also recorded in order to know the stability of the offset voltage at the room temperatures. Offset voltage drift was observed to be maximum of 200 µV. Offset voltage drift is presented in Figure 13 (a) and (b) for PDMS based, and ZnO/PDMS based pressure sensor respectively.

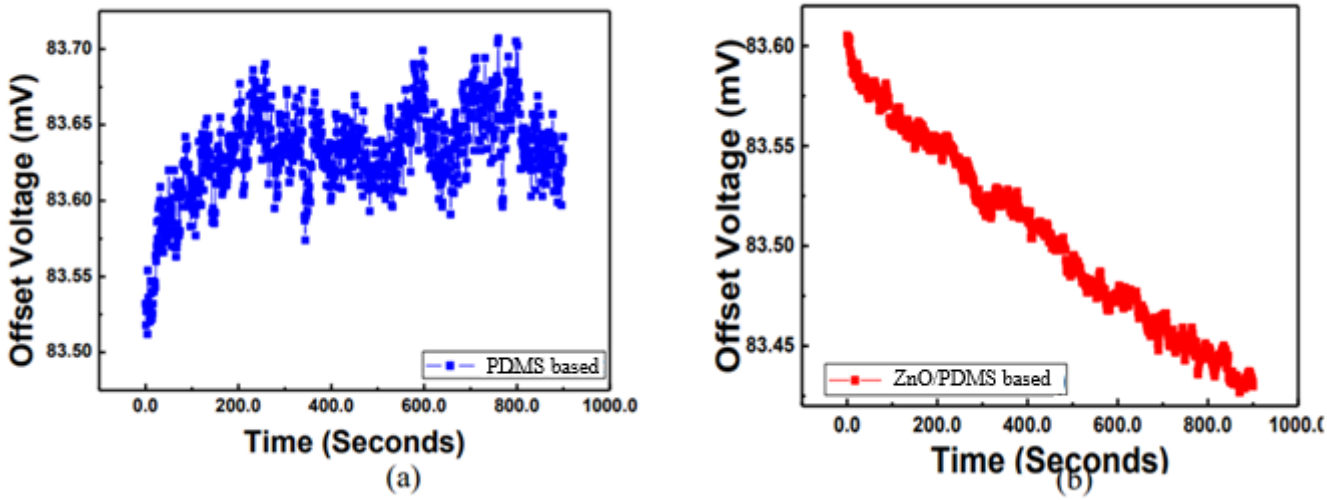

Figure 13: Offset voltage drift at room temperatures for 900 seconds for (a) PDMS based, and (b) ZnO/PDMS based pressure sensor.

Linearity

R square values obtained by linear curve fitting is a measure of the linearity. The linearity of pressure response was very good i. e. R^2~1.The variation in the linearity under the elevated temperatures was found be insignificant. The Figure 14 (a) and (b) shows the linearity (R^2) for PDMS based, and ZnO/PDMS based pressure sensors.

International Journal of Engineering Research & Technology (IJERT)
ISSN: 2278-0181
Vol. 15 Issue 02 , February - 2026

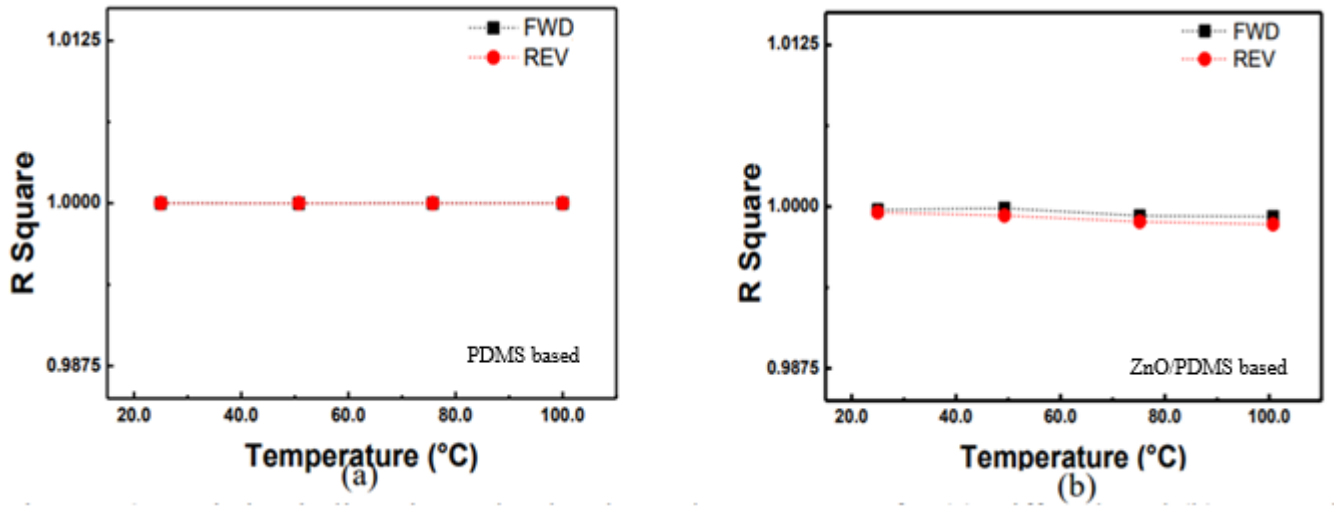

Figure 14: Variation in linearity under the elevated temperatures for (a) PDMS based, and (b) ZnO/PDMS based pressure sensors.

Hysteresis

Hysteresis of the piezoresistive pressure sensors was calculated using the forward and backward pressure response. For each temperature, a forward and backward pressure scan is taken and the hysteresis is calculated from this data. Figure 15 (a) and (b) show variation in hysteresis under high temperatures for PDMS based, and ZnO/PDMS based pressure sensor respectively.

Resistance vs temperature

The gradual increase in the resistance of the surface piezoresistors was observed with temperature. The summarised results of change in the resistance under high temperature are presented in Figure 16 (a) and (b) for PDMS based, and ZnO/PDMS based pressure sensors. The change in the resistance was ~ 6 % and 1.4 % for (a) PDMS based, and (b) ZnO/PDMS respectively.

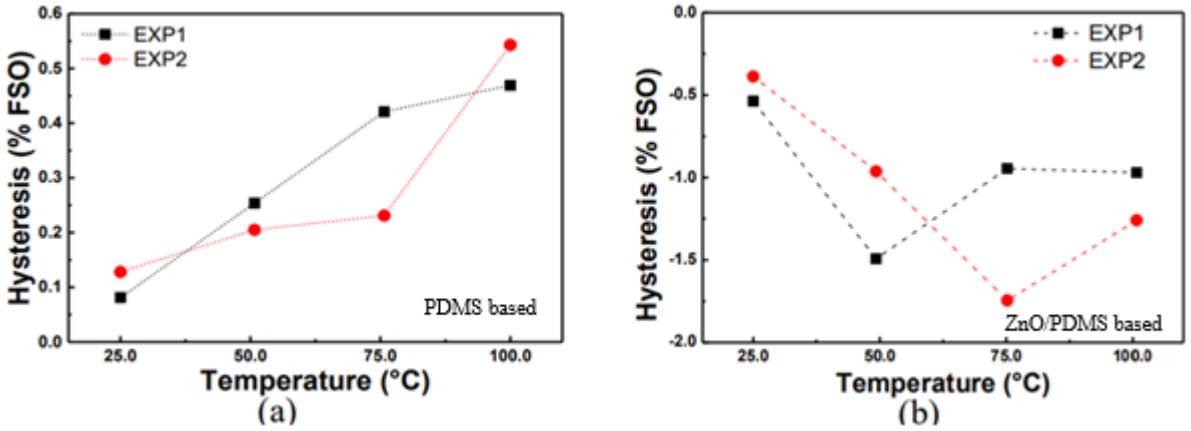

Figure 15: Variation of hysteresis under elevated temperatures for ((a) PDMS based, and (b) ZnO/PDMS based pressure sensors.

International Journal of Engineering Research & Technology (IJERT)
ISSN: 2278-0181
Vol. 15 Issue 02 , February - 2026

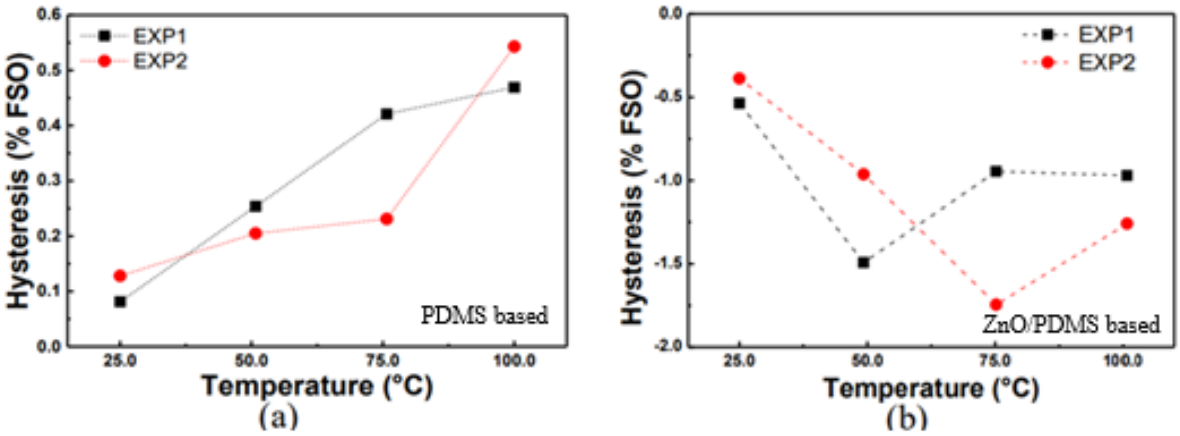

Figure 16: Resistance vs temperature for (a) PDMS based, and (b) ZnO/PDMS based pressure sensors.

Table 2: Summary of performance parameters of developed piezoelectric pressure sensors.

Type	**PDMS based sensors**		**ZnO/PDMS based sensors**		**ZnO/PDMS based sensors**	
Parameters	25ºC	100ºC	25ºC	200ºC	25ºC	200ºC
Sensitivity (mV/V/bar)	0.147	0.127	0.212	0.170	0.186	0.147
Offset (mV)	-16.024	-10.543	-480.56	-518.27		
Hysteresis (% FSO)	0.0543	5.342	0.3089	1.92		
Linearity (R^2)	0.9998	0.999	0.999	0.999		
Range (bar)	200		200		200	200

Conclusion

Thus the fabricated pressure sensor with different weight percentages with PDMS polymer matrix to form ZnO/PDMS nanocomposites while compared with other wt. % ratios. Then the mask design of the pressure sensor was presented in order to fabricate the mask for pressure sensor development. In order to compensate offset voltage and to obtain 4-20 mA response, the design, fabrication and testing were carried out. The operation of this circuit was demonstrated using a commercial pressure sensor which was not having its own signal conditioning circuit. The performance parameters are investigated in terms of the sensitivity, offset voltage, offset drift, linearity and hysteresis.

References

[1] Z.L. Wang, ACS Nano. **7** (2013) 9533–9557.
[2] S.K. Ghosh, T.K. Sinha, B. Mahanty, D. Mandal, Energy Technol. **3** (2015) 1190–1197.
[3] X. Zhang, X. Huang, C. Li, H. Jiang, Adv. Mater. **25** (2013) 4093–4096.
[4] Z. Zhang, J. He, T. Wen, C. Zhai, J. Han, J. Mu, W. Jia, B. Zhang, W. Zhang, X. Chou,C. Xue, Nano Energy. **33** (2017) 88–97.
[5] W. Seung, H.J. Yoon, T.Y. Kim, H. Ryu, J. Kim, J.H. Lee, J.H. Lee, S. Kim, Y.K. Park,Y.J. Park, S.W. Kim, Adv. Energy Mater. **1600988** (2016) 1–8.
[6] B. Kumar, S.-W. Kim, J. Mater. Chem. **21** (2011) 18946.
[7] M. Di Paolo Emilio, Microelectronic circuit design for energy harvesting systems, Springer, 2016.
[8] R. Saidur, N.A. Rahim, M.R. Islam, K.H. Solangi, Renew. Sustain. Energy Rev. **15**(2011) 2423–2430.
[9] R. Tiwari, N.R. Babu, Renew. Sustain. Energy Rev. **66** (2016) 268–285.
[10] T. Quan, Y. Wu, Y. Yang, Nano Res. **8** (2015) 3272–3280.
[11] H. Liu, Y. Xia, T. Chen, Z. Yang, W. Liu, P. Wang, L. Sun, IEEE Sens. J. **17** (2017) 3853–3860.
[12] J. Chen, G. Zhu, W. Yang, Q. Jing, P. Bai, Y. Yang, T.C. Hou, Z.L. Wang, Adv. Mater.**25** (2013) 6094–6099.
[13] Z.L. Wang, G. Zhu, Y. Yang, S. Wang, C. Pan, Mater. Today. **15** (2012) 532–543.
[14] M. Ma, Z. Kang, Q. Liao, Q. Zhang, F. Gao, X. Zhao, Z. Zhang, Y. Zhang, Nano Res.**11** (2018) 2951–2969.
[15] F.R. Fan, Z.Q. Tian, Z. Lin Wang, Nano Energy. **1** (2012) 328–334.
[16] J. Wang, H. Zhang, Y. Xie, Z. Yan, Y. Yuan, L. Huang, X. Cui, M. Gao, Y. Su, W. Yang, Y. Lin, Nano Energy. **33** (2017) 418–

International Journal of Engineering Research & Technology (IJERT)
ISSN: 2278-0181
Vol. 15 Issue 02 , February - 2026

426.
[17] Y. Yang, G. Zhu, H. Zhang, J. Chen, X. Zhong, Z.H. Lin, Y. Su, P. Bai, X. Wen, Z.L. Wang, ACS Nano. **7** (2013) 9461–9468.
[18] X. Fan, J. He, J. Mu, J. Qian, N. Zhang, C. Yang, X. Hou, W. Geng, X. Wang, X. Chou, Nano Energy. **68** (2020) 104319.
[19] X. Wang, S. Wang, Y. Yang, Z.L. Wang, ACS Nano. **9** (2015) 4553–4562.
[20] W. Li, H. Guo, Y. Xi, C. Wang, M.S. Javed, X. Xia, C. Hu, RSC Adv. **7** (2017) 23208– 23214.
[21] Q. Jiang, B. Chen, K. Zhang, Y. Yang, ACS Appl. Mater. Interfaces. **9** (2017) 43716–43723.
[22] Y. Xie, S. Wang, L. Lin, Q. Jing, Z.H. Lin, S. Niu, Z. Wu, Z.L. Wang, ACS Nano. **7**(2013) 7119–7125.
[23] G. Zhu, Y. Su, P. Bai, J. Chen, Q. Jing, W. Yang, Z.L. Wang, ACS Nano. **8** (2014) 6031–6037.
[24] G. Zhu, Y. Su, P. Bai, J. Chen, Q. Jing, W. Yang, Z.L. Wang, ACS Nano. **8** (2014) 6031–6037.
[25] X. Yang, S. Chan, L. Wang, W.A. Daoud, Nano Energy. **44** (2018) 388–398.
[26] A. Ahmed, Z. Saadatnia, I. Hassan, Y. Zi, Y. Xi, X. He, J. Zu, Z.L. Wang, Adv. Energy Mater. **7** (2017).
[27] Z. Saadatnia, E. Asadi, H. Askari, J. Zu, E. Esmailzadeh, Int. J. Energy Res. (2017) 1– 13.
[28] Y. Su, X. Wen, G. Zhu, J. Yang, J. Chen, P. Bai, Z. Wu, Y. Jiang, Z. Lin Wang, Nano Energy. **9** (2014) 186–195.
[29] X. Wang, B. Yang, J. Liu, C. Yang, J. Mater. Chem. A Mater. Energy Sustain. **5** (2017) 1176–1183.
[30] C. Cui, X. Wang, Z. Yi, B. Yang, X. Wang, X. Chen, J. Liu, C. Yang, ACS Appl. Mater. Interfaces. **10** (2018) 3652–3659.